ISBN: 978-3-95450-247-9 ISSN: 2673-5490 doi: 10.18429/JACoW-IPAC2024-THPR17

DIMENSIONAL AND THERMAL DESIGN OF THE ELECTROSTATIC CHOPPER FOR THE NEW ISIS MEBT

I. Rodriguez†, S. Lawrie, J. Speed, ISIS, Rutherford Appleton Laboratory, STFC, Didcot, UK

Abstract

The electrostatic chopper for the new ISIS MEBT is a fast deflecting device to create gaps in the beam coming out of the RFQ, which will improve the trapping efficiency when injecting the beam into the ISIS synchrotron. The electromagnetic design of the chopper was initially developed to define its functional specifications, shape and dimensions, and it was presented elsewhere. A dimensional sensitivity study was developed to estimate the maximum acceptable thermal loads due to the beam loss (used later in the thermal model) and to ensure that the electric field shape and strength were still valid. Dimensional tolerances were defined based on the sensitivity study. Thermal calculations and models were required to ensure that the electrodes were properly cooled for the expected beam loss in the diverse working and failure situations, and to ensure that the hot beam dump inside the chopper was not indirectly overheating the electrodes. The mechanical design and manufacturing were carried out according to the results from the previous analyses, and the details are presented elsewhere.

SENSITIVITY AND TOLERANCES

The MEBT chopper is required to clean the leading edge of the H^- beam between the RFQ and the DTL in the ISIS LINAC, and to burst-chop the beam into shorter pulses to improve efficiency. A full electromagnetic design was developed in [1] to define the chopper design parameters and its functional specifications. A calculation of the discarded beam averaged powers resulted in 197.6 W for the maximum required 40% burst chopping of the beam. However, in a failure scenario where all the beam is dumped to the beam dump, the dissipated beam power would be 407 W.

The largest source of heating in the chopper is the beam loss, not the pulsed EM wave travelling through it, which was estimated to be in the order of a few milliWatts [1]. The electrodes experience the largest beam loss after the beam dumps. It is critical to estimate the heat loss on the electrodes, as it is a technical challenge to extract the heat of electrically insulated parts inside a vacuum.

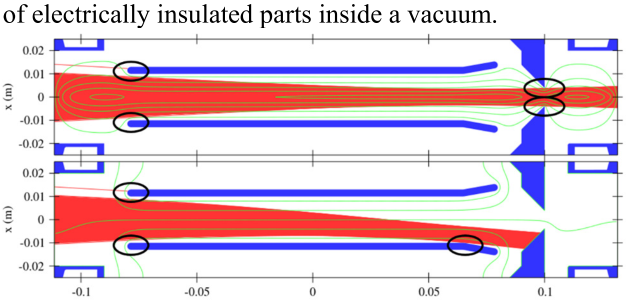

Figure 1: High beam loss areas in the chopper.

The electrodes can scrape the beam during the OFF and ON chopper states, at the leading ends and at the ends closer to the dumps respectively (see Fig. 1). Identically, the beam dumps can scrape the beam during the OFF chopper state, although that can be minimised during the commissioning by adjusting the dump positions.

The positioning tolerance of the electrodes relative to the beam has two effects: it changes the electric field between the electrodes (altering the beam position on the beam dump) and it increases/decreases the amount of beam scraped by the electrodes (adding more heat loss to the electrodes). The former was studied for a sensibly large gap tolerance of ±1 mm, and it showed a negligible change in the beam position on the beam dump. The latter was more sensitive to the electrode positioning tolerances, either risking the device integrity or requiring too tight tolerances, which in fact triggered the design change from a flat electrode shape to a "flared" end electrode shape.

The percentage of the beam that hits the electrodes was calculated by beam tracking simulations [2] for under-focused, nominal and over-focused beams, both in ON and OFF chopping states, and for 3 different electrode misalignment cases (each one for a symmetric and asymmetric misalignment): Transverse (±1 mm gap), longitudinal (±1 mm) and rotational (±7 mrad) misalignments. The transverse misalignment resulted in a worst case beam loss on one electrode of less than 0.8% of the beam (1.6 W) for the symmetric offset, under-focused beam (Fig. 2). The rotational misalignment loss was up to 0.3% of the beam (0.6 W) for a big rotation of 7 mrad per electrode (vs. the mid-plane). The worst beam loss for the longitudinal misalignment case was less than 0.1 W.

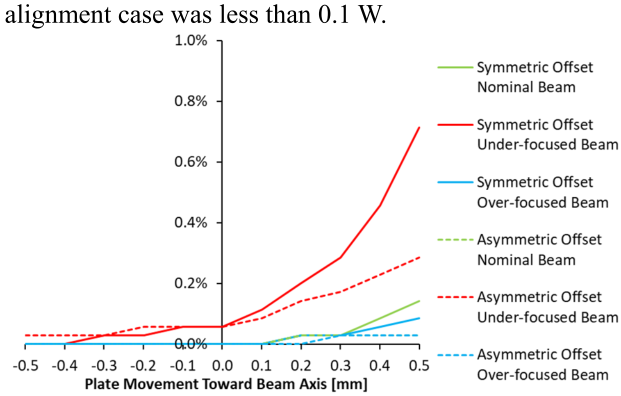

Figure 2: Transverse electrode misalignment case.

This study returned a set of recommended mechanical tolerances (Table 1) and several conclusions:

- The longitudinal electrode positioning is not critical for the beam loss.
- The rotational misalignment in the direction of the deflected beam should be favoured to reduce beam loss.

† iker.rodriguez@stfc.ac.uk

ISBN: 978-3-95450-247-9 ISSN: 2673-5490 doi: 10.18429/JACoW-IPAC2024-THPR17

- The transverse misalignment tolerance should be defined to increase the gap between the electrodes.
- The theoretical beam axis (vertical mid-plane) should be referenced to an external feature for alignment.

Table 1: Summary of the Recommended Tolerances

Description	Nominal value	Tolerance	Units
Distance from each electrode (inner surface) to the vertical mid-plane.	10	+0.5 / +0	mm
Distance from electrode straight section end to beam dumps.	25.4	±1	mm
Length of straight section of electrodes.	144.6	+0 / −1.5	mm
Distance from electrode ends to upstream flange face.	31.5	+0 / −0.5	mm

THERMOMECHANICAL MODEL

Electrode cooling

The maximum estimated beam loss on the electrodes was 1.6 W, as it was presented in the previous section. That value was used for the subsequent thermomechanical models. A quick hand calculation using Fourier's law of conduction showed that the electrodes could be safely cooled down by conduction to the vessel, avoiding challenging water cooling systems inside vacuum and high voltage. It was estimated that the electrode temperature increment between the ceramic supports should be limited to about 20 ºC to avoid electrode warping, so the tolerances in the bolt holes used for one of the supports (the other was counter-bored to keep it fixed) could accommodate for the thermal expansion.

The conduction cooling imposed for the electrodes required a good contact between the different interfaces (electrodes to insulators and insulators to vessel). The thermal contact resistance would dominate the heat transfer mechanism if the contact between surfaces was poor. The effect is exacerbated by the high vacuum, which removes the interstitial gas between the microscopic peaks and valleys. The true contact area between two surfaces can be very small, usually less than 1% of the nominal surface area, and typically between 0.1 and 0.2% [3]. It depends on the surface finish, the contact pressure and the micro hardness of the surfaces. This was estimated by using mock-up tests [4] and analytical correlations like the Cooper-Mikic-Yovanovich (CMY) [5]. Assuming a surface roughness Ra=1.6 µm and only 0.1% of the area in actual contact (worst case scenario), the specific contact resistance between the insulators and the electrodes (Shapal™ to aluminium) was 2.535 x 10^{-5} K.m^2/W. Using the same assumptions between the insulators and the vessel (Shapal™ to steel), the value was 1.241 x 10^{-4} K.m^2/W. These specific contact resistances were very similar when calculated using the CMY correlation in test FEM models using sensible surface finishes (Ra=1.6 µm), contact pressures (750 kPa) and documented material microhardness (~1 GPa) [6], and they were used both in subsequent analytical and FEM models to estimate the electrode temperatures.

A simple spreadsheet was produced to calculate the electrode expansion when the estimated contact resistances are included. The result was a total thermal resistance (from the electrode tip to the vessel) of 3.11 K/W. That produced a temperature increase of 4.92 °C from the electrode end tip to the vessel external surface, for 1.6 W beam loss. The expected electrode expansion between supports for a 28 °C external vessel temperature was 13.5 µm (also see 3D FEM model results), easily accommodated by the tolerance of the bolts without any warping in the electrodes.

Beam dump cooling

The power dissipated by the dumped beam was about 198 W minus the beam lost on the electrodes. The tungsten end was bolted to a water cooled copper heat sink to extract the heat. A coaxial cooling system was used due to constraints on the available space and to minimise the length of the conduction path (Fig. 3). Different methods were considered to finely tune the distance between the tungsten tip and the beam axis in 0.1 mm steps. A shimmed positioning system between the tungsten and the copper [7] was finally selected for its simplicity, and its definitive thickness will be selected during the beam commissioning process.

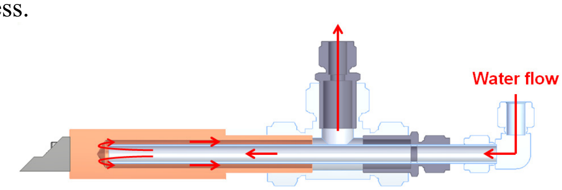

Figure 3: Beam dump cooling circuit.

A spreadsheet was produced to analytically calculate the required water flow rate and the temperatures in a simplified model of the beam dump, when 196 W were dissipated on it. The result predicted a maximum temperature of 162 °C for the beam dump, with a water flow of 15.6 l/min. The local water speed was checked by a CFD model of the beam dump cooling system (Fig. 4), which also confirmed the calculated convective heat transfer coefficients.

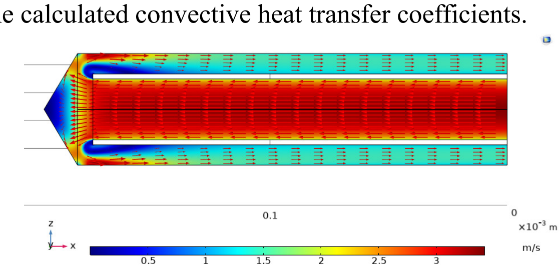

Figure 4: RANS k-ε turbulence model for a beam dump.

Full FEM 3D model

A FEM 3D model with the final geometry of the chopper was developed in COMSOL Multiphysics [8] (Fig. 5). The model included a coupled multiphysics study of the fluid

ISBN: 978-3-95450-247-9 ISSN: 2673-5490 doi: 10.18429/JACoW-IPAC2024-THPR17

flow in the beam dumps, the thermal conduction and convection in the fluids and solids and the structural deformations due to the material thermal expansion. Thermal radiation was also studied between the parts inside the chopper, but was found to be negligible (as initially predicted).

Several working cases were solved to obtain the working temperatures and the displacements of the structure. Two equipment failure scenarios were also studied, one with the un-chopped beam being dumped to one beam dump (e.g. due to a switch locked at DC voltage), and other with the beam fully hitting one electrode (e.g. due a too high deflecting voltage).

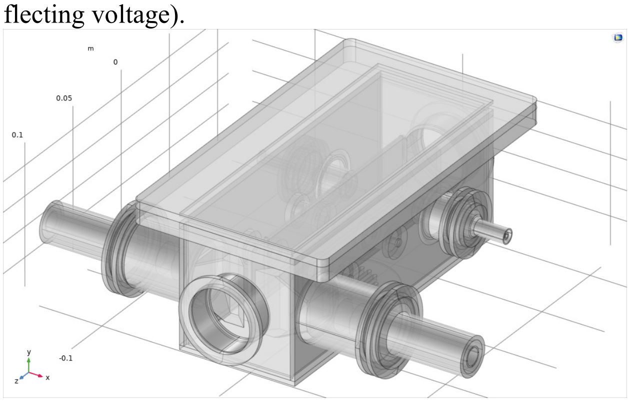

Figure 5: Thermomechanical model geometry.

A summary of the results is shown in Fig. 6, where colours visually score the risk for each scenario (green-OK, yellow-Risky, red-Dangerous). The absolute temperature results were based on a cooling water temperature of 20 °C at a constant flow rate of 15.6 l/min, and an ambient temperature of 20 °C. It is worth noticing how close the analytical and the FEM results were for the nominal working case. In addition, the thermal results clearly showed that very small beam losses on the electrodes could become dangerous, while the beam dumps are more resistant to operation mistakes (limited only by the boiling temperature of the cooling water at the heatsink).

	One beam dump (analytic)	One beam dump (FEM)	Both beam dumps	Full beam to one beam dump	Full beam to one electrode
Power on beam dump(s)	196 W		98 W	404 W	0 W
Power on electrode(s)	1.6 W		0.79 W	3.26 W	197.6 W
ΔT electrode(s) end hotspot to vessel wall	4.9 °C	4.5 °C	2.2 °C	9.3 °C	485 °C
T at electrode(s) end (near dump)	32.9 °C	32.5 °C	27.6 °C	44.6 °C	N/A - Melt
T at beam dump(s) tip	162 °C	160 °C	88 °C	326 °C	20.5 °C
Electrode ΔL between supports	13.5 µm	11.8 µm	7.5 µm	23 µm	N/A

Figure 6: Chopper temperatures.

The results of the structural analysis for the first working case in Fig. 6 are shown in Fig. 7. The hot electrode expands by 11.8 µm between the insulating supports, not far off of the analytically calculated value. The supports are solidly fixed to the electrodes and the vessel in the model, so the structure is more rigid than in reality, and therefore the calculated deformation and shape are not totally accurate. However, the absolute deformation values are so small that the thermal expansion should not represent any problem for the structure or the feedthrough pin.

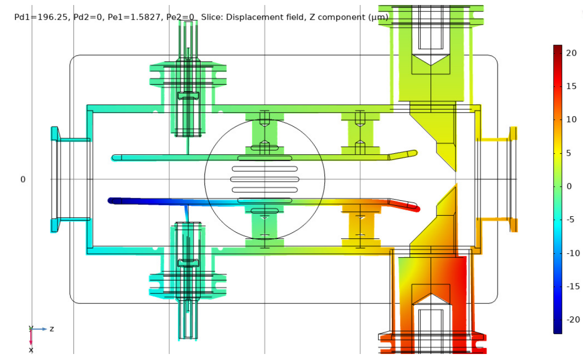

Figure 7: Chopper deformations on Z axis (µm).

To avoid and/or detect operation mistakes leading to the studied failure scenarios, the power supply voltage should be hard limited and several thermal sensors should be added to monitor the vessel and the beam dump temperatures, including triggering values for warning and switch off conditions, as shown in Fig. 8. The electrode temperature can also be directly monitored by including an insulated optical thermal probe inside the electrodes [9].

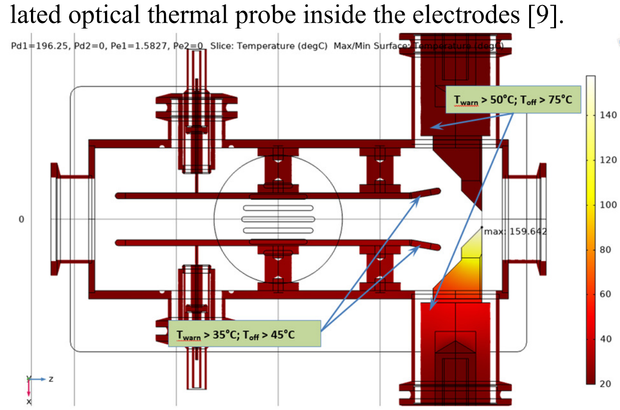

Figure 8: Chopper temperatures and sensor settings.

CONCLUSION

The dimensional and thermal design of an electrostatic chopper for the new ISIS MEBT has been presented, including the sensitivity and tolerance analysis and the cooling calculations. The calculated tolerances were mainly determined by the beam loss on the electrodes, and the recommended values were quite loose for a device of these dimensions. However, the contact between the electrodes and the ceramic stand-offs and vessel was shown to be critical to achieve a low thermal contact resistance, which will require a quite good surface finish and alignment for the surfaces in contact.

The thermo-mechanical model showed a very good agreement between the analytical and FEM calculations for the nominal working case, and the thermal results indicated a safe operation even if the full beam was accidentally dumped to only one of the beam dumps. Continuously dumping the beam on one electrode would damage the chopper, hence why it is crucial to have temperature sensors interlocked to the beam and/or the power supply. It is recommended to drive the power supply in alternating polarity during the burst chopping mode to alleviate the beam heat load both on the beam dumps and on the electrodes.

ISBN: 978-3-95450-247-9 ISSN: 2673-5490 doi: 10.18429/JACoW-IPAC2024-THPR17

REFERENCES

[1] I. Rodriguez, S. Lawrie and J. Speed, “Design of an Electrostatic Chopper for the New ISIS MEBT”, in *Proc. IPAC'23*, Venice, Italy, May 2023, pp. 2194-2197, doi:10.18429/jacow-ipac2023-tupm016

[2] S. Lawrie, “Chopper tracking simulations for mechanical tolerances - Internal report”, Rutherford Appleton Laboratory, UK, 2019.

[3] J. Dyson and W. Hirst, “The True Contact Area Between Solids,” in *Proc. Phys. Soc. B,* vol. 67, pp. 309-312, 1954.

[4] I. Rodriguez, “Chopper for the ISIS MEBT – Technical Design Report - Internal report”, Rutherford Appleton Laboratory, UK, Sep. 2020.

[5] M. M. Yovanovich, “New Contact and Gap Correlations for Conforming Rough Surfaces”, *AIAA 16th Thermophysics Conference*, Palo Alto, CA, 1981.

[6] M. M. Yovanovich, “Four Decades of Research on Thermal Contact, Gap, and Joint Resistance in Microelectronics”, in *IEEE Transactions on Components and Packaging Technologies,* vol. 28, no. 2, June 2005.

[7] J. Speed and A. Lees, “Chopper for the ISIS MEBT - Mechanical design report - Internal report”, Rutherford Appleton Laboratory, UK, 2020.

[8] COMSOL AB, “COMSOL Multiphysics® software”, https://www.comsol.com

[9] J. Speed, A. Avaroglu and I. Rodriguez, “Practical design and manufacturing of the new ISIS MEBT chopper”, presented at IPAC'24, Nashville, USA, May 2024, paper THPR021, this conference.